p-ISSN: 2301-6663, e-ISSN: 2477-250X
URL: http://ojs.ummetro.ac.id/index.php/turbo

Numerical Method To Overcome The Fluid Flow Separation On Pipe Bend 90° Using Guide Vane

Khalees Sedeq[1], James Julian[2*], Fitri wahyuni[3], Waridho Iskandar[4]

[1-3]Teknik Mesin, Fakultas Teknik, Universitas Pembangunan Nasional Veteran Jakarta Jalan RS. Fatmawati Raya, Pd. Labu, Kec. Cilandak, Kota Depok, Jawa Barat, Indonesia
[4]Fluid Mechanics Laboratory, University Indonesia, Kampus Baru UI, Depok 16424, Jawa Barat, Indonesia
**Corresponding author*: zames@upnvj.ac.id

Abstract

This research delves more profoundly into examining fluid flow within a 90° pipe bend. Computational computations are executed utilizing the Reynolds-Averaged Navier-Stokes (RANS) equations. More precisely, this investigation utilizes the K-ε turbulence model. The present study employs a grid with the most elements used, chosen for its minimal error value. The central objective of this research revolves around mitigating flow separation by integrating a guide vane to modify the fluid flow attributes within a 90° pipe bend, with a curvature ratio $\frac{R_c}{D} = 1$. In this instance, the pipe has a diameter of 0.01 m. When examining the 90° pipe bend without a guide vane, it becomes evident that flow separation occurs in the inner core region, and the maximum velocity region is situated in the outer core area. In contrast, when utilizing a guide vane in the 90° pipe bend, the fluid flow is directed more uniformly among the outer and inner core regions. Additionally, there is no identifiable low-velocity region where the guide vane is employed. Consequently, a guide vane effectively alleviates flow separation in the 90° pipe bend. Additionally, this study investigates various Reynolds numbers, namely 6×10^4, 7×10^4, and 8×10^4. Increasing the Reynolds number does not significantly affect the velocity profile. However, it significantly influences the separation angle (α), with higher Reynolds numbers leading to larger α values. Furthermore, increasing the Reynolds number results in an earlier reattachment point in the 90° pipe bend without a guide vane.

***Keywords*:** pipe bend, separation, guide vane, Reynolds number

1. Introduction

A fluid is a substance capable of undergoing continuous transformation when exposed to force or shear stress. Fluid flow is categorized into two distinct groups depending on its boundary conditions. [1]–[3]. The first category is external fluid flow. External flow is the flow of fluid that freely moves without being constrained by a solid surface. Some applications of external fluid flow include parachuting, airflow around vehicles, water flow around a submarine, and others [4], [5]. The second category is internal fluid flow. Internal flow is defined as the flow of fluid that is confined by solid surfaces. Internal fluid flow is widely applied, especially in water distribution within a piping system [6]. The shape and selection of pipes significantly influence the flow conditions within a pipe [7], [8]. The fluid flow characteristics in straight pipes are, of course, different from those in pipe bends. One common type of pipe bend used is the 90° pipe bend. This pipe bend is a crucial component within piping systems. A 90° pipe bend provides flexibility in fluid distribution [9], [10]. Various fluid flow phenomena can be observed within a 90° pipe bend, including instability, separation, and secondary flow [11], [12]. The Reynolds number typically influences all these phenomena, the flexion ratio of the pipe bend, and the pipe diameter [13].

Research on fluid flow within pipes is intriguing to investigate. Analysis can be conducted using various methods, such as experimental, numerical, and theoretical approaches. [14] An experimental study is undertaken to analyze turbulent flow in a 90° pipe bend with a bend ratio $\frac{R_c}{D} = 2$. A linear pipe segment is constructed with a length of 100 times the pipe diameter (100D) and positioned upstream of the bend to ensure the delivery of fully developed

DOI: http://dx.doi.org/10.24127/trb.v12i2.2846
Received 27 September 2023; Received in revised form 17 December 2023; Accepted 18 December 2023
Available online 31 December 2023

turbulent flow into the pipe bend. The experiment employs air as the working fluid with a Reynolds number of 60000. The research presents findings regarding phenomena occurring along the pipe's length and within the pipe bend (α=30°), where secondary flow develops into a pair of vortices. Flow velocity and circumferential velocity measurements at various locations along the pipe are conducted using a hot-wire anemometer. [15] In an investigative study focusing on a 90° pipe bend, the k-epsilon turbulence model equation was employed as a turbulence model to investigate the impact of varying Reynolds numbers. The study's results demonstrate that with an increase in the Reynolds number, a wholly developed velocity profile becomes evident within the inner core region of the pipe bend. Furthermore, the elevation in Reynolds number influences the occurrence of fluid flow separation inside the pipe. With an increasing Reynolds number, the separation point moves nearer to the upstream portion. Conversely, an increase in Reynolds number results in the reattachment point shifting closer to the downstream segment. Additionally, a low-velocity zone was identified within the inner core region of the conduit, signifying the initiation of fluid flow separation. [16] In experimental and computational studies on a 90° pipe bend with turbulent flow, similarities in fluid velocity profiles are observed within the Reynolds number range of 5×10^4 to 2×10^5.

In general, numerous inquiries have been conducted regarding 90-degree pipe bends. Typically, these investigations focus more on the effects of variations in Reynolds number and curvature ratio in 90-degree pipe bends without delving further into the underlying phenomena. Previous studies suggest fluid flow separation occurs when $\frac{R_c}{D} \leq 1.5$, where R_c denotes the curvature of the pipe bend and D is the pipe diameter. This can lead to hydraulic losses in the fluid flow through the pipe. There is a relative scarcity of research explicitly addressing measures to alleviate fluid flow separation in 90-degree pipe bends. Therefore, this study aims to address the phenomenon of flow separation in 90-degree pipe bends with a curvature ratio of $\frac{R_c}{D} = 1$ by optimizing the design of the 90-degree pipe bend with guide vanes to enhance fluid flow efficiency. This research will also uncover the fluid flow characteristics inside the 90-degree pipe bend with guide vanes, examining features such as velocity profiles, streamlines, and fluid flow contours.

Methodology

1. Geometry simulation

This research conducts fluid flow simulations within a pipe with a 90° bend angle. The simulations are performed using the Fluent software as the computational tool. The study is focused on a pipe bend ratio $\frac{R_c}{D} = 1$, with a diameter (D) of 0.01 m. Two geometries are employed in this study. The first geometry is a pipe bend without a guide vane. The second geometry is a pipe bend with a guide vane along its length. The upstream side of the 90° pipe bend has a length of 50D, while the downstream side has a length of 20D [10]. Refer to the geometry depicted in Figure 1.

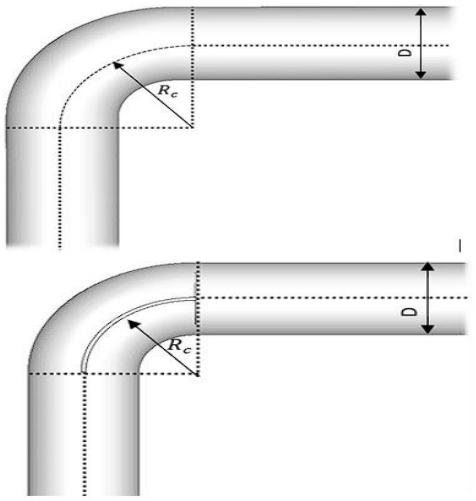

Figure 1(a) depicts a pipe bend without guide vane, while Figure 1(b) illustrates a pipe bend 90° using guide vane

2. Guide vane

The guide vane is one of the components widely used in various pumps, compressors, or turbines. The primary function of the guide vane is to alter or divide the fluid flow. Guide vanes typically consist of one or more blades positioned along the path of fluid distribution. When the fluid passes through the guide vane, the flow is divided as the fluid interacts with the side of the guide vane, allowing flow division [17]. The mechanism of the guide vane in preventing separation in a 90° pipe bend involves dividing the fluid flow horizontally to prevent separation on the inner core side. Additionally, the guide vane directs and stabilizes the fluid flow to prevent it from transitioning into turbulent flow, thereby preventing flow separation in the pipe bend [18]. The guide vane also maintains the stability of fluid flow velocity, preventing fluctuations in fluid flow velocity. In this study, the guide vane is employed by modifying the geometry of the 90° pipe bend to mitigate flow separation occurring at a pipe bend. The pipe diameter is 2.5 times larger than the thickness of the guide vane, where the guide vane in this study has a thickness of 0.0004 m and a width of 0.01 m. The guide vane is horizontally positioned within the pipe bend, and its shape is depicted in Figure 2 [17]. Figure 2 illustrates the form of the guide vane.

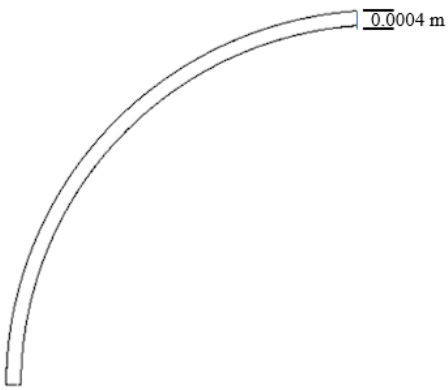

Figure 2 illustrates the shape of the guide vane

3. Meshing

Mesh is one of the fundamental elements in the simulation process that are interconnected to form a network. Mesh is used to divide the physical domain into smaller parts. Mesh enables mathematical modeling and the discrete solution of differential equations. The research employs a mesh of three-dimensional elements structured using a hexahedral model. The advantage of utilizing the mesh is its consistency, which streamlines the computational domain's structure, enhancing computational efficiency and diminishing iteration expenses [19]. In this research, three mesh configurations were generated, each differentiated by the quantity of elements. Specifically, these configurations comprised 500,000 elements, 1 million elements, and 2 million elements. The choice of the most suitable mesh for further investigations was determined through the outcomes of the mesh independence assessment. Figure 3 visually represents the mesh configurations employed in this study.

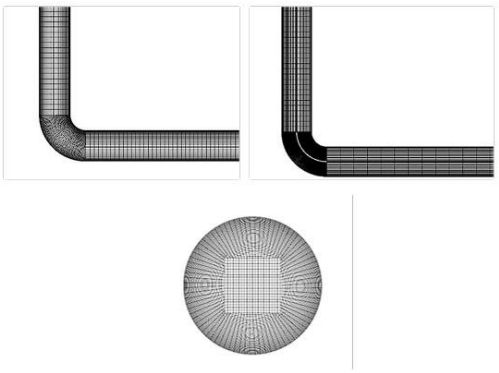

Figure 3 (a) depicts the mesh without a guide vane, 3(b) the mesh with a guide vane, and 3(c) the mesh on the pipe surface.

4. Reynolds number

The Reynolds number is a dimensionless quantity employed to characterize the nature of fluid motion. Typically, the Reynolds number refers to flow conditions where a higher value of

the Reynolds number determines the type of flow occurring in the working fluid [20]. In this research, the Reynolds number used varies to ascertain the effects of increasing the Reynolds number. The Reynolds numbers used in the study are $6 \times 10^4, 7 \times 10^4,$ and 8×10^4.

$$R_e = \frac{\rho\, v\, d}{\mu} \quad (1)$$

where ρ= density ($\frac{kg}{m^3}$), v = kinematic viscosity ($\frac{kg}{m-s}$), d = pipe diameter (m) dan μ= viskositas (pa)

5. Governing equation

In the numerical methodology for addressing fluid flow scenarios within a pipe bend, the Reynolds-Averaged Navier-Stokes (RANS) equations are utilized. The U-RANS equations are computed using a second-order method, and the relationship between pressure and velocity is established using the COUPLED algorithm. In this ongoing study, a time step of 0.001 seconds is utilized, resulting in 1000-time steps. Predefined relaxation factors are employed to aid in achieving convergence across all models. The fluid used in this research is water with a dynamic viscosity (μ) of 0.0006 $\frac{kg}{m-s}$ and density (ρ) of 990.2 kg/m^3. The RANS equations in this study model incompressible flow, as there is no need to consider changes in density in the equations, where density remains constant. Typically, the RANS equations comprise two fundamental equations for incompressible flow: the continuity equation and the momentum equation. [15]. The mass conservation equation can be observed in Equation 2, while the momentum conservation equation can be found in Equation 3.

$$\frac{\partial u_i}{\partial x_i} = 0 \quad (2)$$

$$\frac{\partial u_i}{\partial t} + u_j \frac{\partial u_i}{\partial u_j} = f_i - \frac{1}{\rho}\frac{\partial p}{\partial x_i} + v\frac{\partial^2 u_i}{\partial x_i \partial x_j} \quad (3)$$

6. Turbulence model

In this investigation, the utilization of simulations at a Reynolds number exceeding 60,000 allows us to assert that the fluid flow within the pipe undergoes turbulence. Consequently, in this research, we incorporate a turbulence model as an adjunct to the RANS equations under turbulent flow characteristics. Various turbulence models are commonly employed within the framework of RANS equations. The choice of an appropriate turbulence model necessitates consideration of several factors, including the flow type, scale, and the desired level of accuracy. This research utilizes the traditional k-ε turbulence model to describe the properties of turbulence in single-flow and two-phase flow [16], [21]. This model addresses the calculation of turbulence kinetic energy (k) and turbulence dissipation rate (ε) to determine the turbulent viscosity coefficient. The transport equations for k and epsilon are employed for this specific objective.

$$\frac{\partial(pk)}{\partial t} + \frac{\partial(pku_i)}{\partial x_i} = \frac{\partial}{\partial x_j}\left[\frac{\mu_t}{\sigma_k}\frac{\partial k}{\partial x_j}\right] + 2\mu_t E_{ij} E_{ij} - \rho\varepsilon \quad (4)$$

$$\frac{\partial(p\varepsilon)}{\partial t} + \frac{\partial(p\varepsilon u_i)}{\partial x_i} = \frac{\partial}{\partial x_j}\left[\frac{\mu_t}{\sigma_\varepsilon}\frac{\partial k}{\partial x_j}\right] + C_{1\varepsilon}\frac{\varepsilon}{k}2\mu_t E_{ij}E_{ij} - C_{2\varepsilon}\rho\frac{\varepsilon^2}{k} \quad (5)$$

In this context, u_i denotes the velocity component in the flow direction, E_{ij} signifies the components of the deformation rate, and μ_t represents turbulent eddy viscosity. Equations 4 and 5 consist of several constants, namely:
$c_\mu = 0.09 \;\; \sigma_k = 1.00 \;\; \sigma_\varepsilon = 1.30$
$C_{1\varepsilon} = 1.44 \;\; C_{2\varepsilon} = 1.92$

7. Tapping line

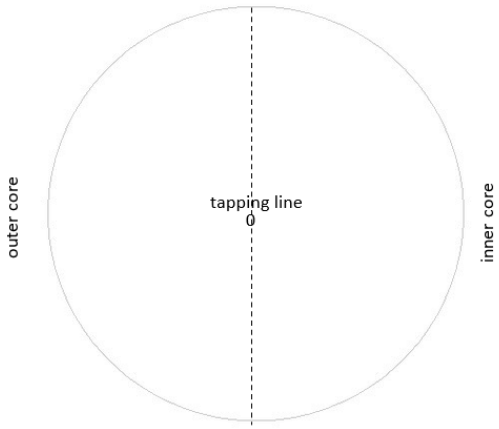

Figure 4 tapping line

The tapping line is the data collection location in this study, as shown in Figure 4[22].

8. Separation flow

In fluid mechanics, flow or boundary layer separation occurs when the boundary layer detaches from the surface[3]. The boundary layer arises whenever relative motion between a fluid and a solid surface, with viscous forces influencing the fluid layer near the surface. This flow can occur externally, around an object, or internally, within a closed channel. Depending on the flow conditions, the boundary layer may exhibit laminar or turbulent characteristics[23]. Separation of the boundary layer in internal flow can be attributed to various factors, such as the rapid expansion of a pipe channel. Separation occurs when adverse pressure gradients develop as the flow expands, forming a separated flow region. The portion of the separate flow is referred to as the separation point, dividing the recirculating flow from the flow passing through the central region of the channel. The point where the separation streamlines reattach to the wall is termed the reattachment point. Generally, flow separation occurs in decelerating flows with increased pressure, especially after passing through the thickest part of the streamline or a widening channel. As the flow progresses downstream, it eventually reaches a state of equilibrium where there is no backflow. A rational assessment of whether the boundary layer will be laminar or turbulent can be made by calculating the Reynolds number under local flow conditions[17].

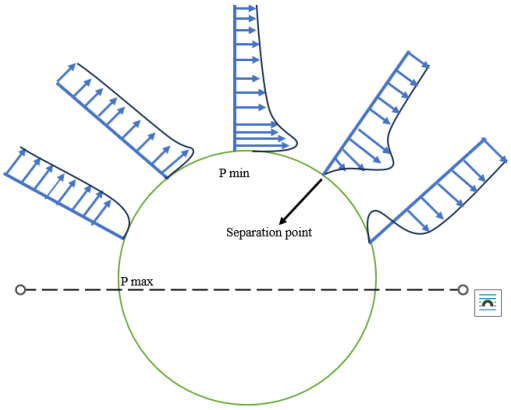

Figure 5 separation point

Result and Analysis

1. Mesh independence test

Mesh independence testing is employed in this study for verification purposes. The utilized approach involves Richardson Extrapolation, and each stage of mesh independence testing is executed following the methodology employed in the Waridho research. The attributes employed in the mesh independence assessment encompass velocity parameters at specific coordinates: $z = 0.02, y = 0, dan\ x = 0$. All variables related to the testing are presented in Table 1. The variations in the number of meshes fall within the conformity index range, where the mesh independence test results are observed $\frac{GCI_{coarse}}{GCI_{fine}(r^p)} \approx 1$. Figure 6 showcases the results of the mesh independence test, revealing a minimal disparity associated with the finer mesh, with an error value of 0.1324%. Therefore, a grid of 2×10^6 is utilized in this study [23].

Tabel 1. Mesh independence test

Mesh group	Total of Elements	Velocity	District code	Error
Fine	2×10^6	3.999	f_1	0.1324%
Medium	1×10^6	3.975	f_2	0.7339%
Coarse	5×10^5	3.841	f_3	4.0687%

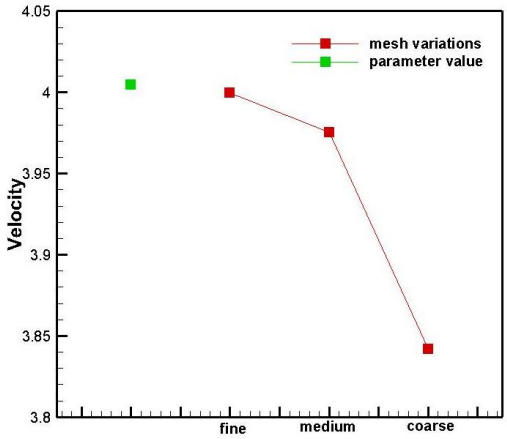

Figure 6 mesh independent test result.

2. Validation

The data gathered in this investigation should undergo validation by comparing the research findings with prior studies or other research endeavors. Data for comparison are derived from the experimental study [16], and the simulation study [15]. The results of data validation are presented more clearly in Figure 7. Data collection was conducted in the pipe simulation with a bend ratio $\frac{Rc}{D} = 2$, and the velocity details was collected at the outlet of the pipe bend. As illustrated in Figure 6, following the validation outcomes, it is evident that the data presented in this research closely corresponds with the

findings of prior investigations. [15], [16], particularly in the range of r/R= -0.49 to r/R=0.49, indicating a good agreement. The trend of the data in this study aligns with the reference studies. However, some validation data points do not align precisely, specifically in the r/R = 0 to r/R=0.3 range. This data variation may occur in the inner core area of the pipe bend, where an unfavorable pressure gradient occurs. As a result, the data collected in this investigation can be deemed reasonably accurate.

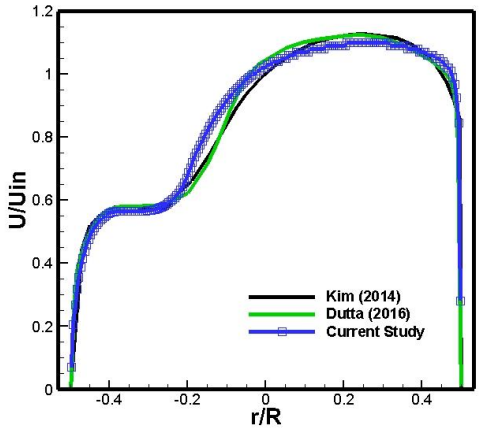

Figure 7 Validation graph with other studies.

3. Research result

By collecting data from the exact validation location, which is at the position of 0.02 downstream (sb) of z at the outlet of the pipe bend for each dataset in this section. The Reynolds numbers for each data are $6 \times 10^4, 7 \times 10^4,$ and 8×10^4. The analysis focuses on velocity profiles, velocity fluctuations, separation, and reattachment locations in the 90° pipe bend without a guide vane, as well as the results after the use of a guide vane in the 90° pipe bend.

Figure 8 illustrates velocity profiles that have been normalized based on the inlet velocity. Among the three Reynolds numbers employed, significant variations in velocity profiles are observed between the 90° pipe bend devoid of a guide vane and the 90° pipe bend by a guide vane. Among the three Reynolds numbers used it can be confirmed that the Reynolds number does not significantly influence the fluid velocity profile. When compared, a guide vane does not significantly change the velocity profile in the -0.5≤r/R≤-0.35 range. Meanwhile, in the range of -0.34≤r/R≤0.05, a guide vane can enhance the fluid velocity profile compared to the 90° pipe bend without a guide vane. Furthermore, in the range of 0.05≤r/R≤0.5, using a guide vane slightly decreases the fluid flow velocity. Using a guide vane also shifts the velocity profile to the position of r/R=-0.07. It contrasts the 90° pipe bend lacking a guide vane, with the highest velocity profile near the outer core.

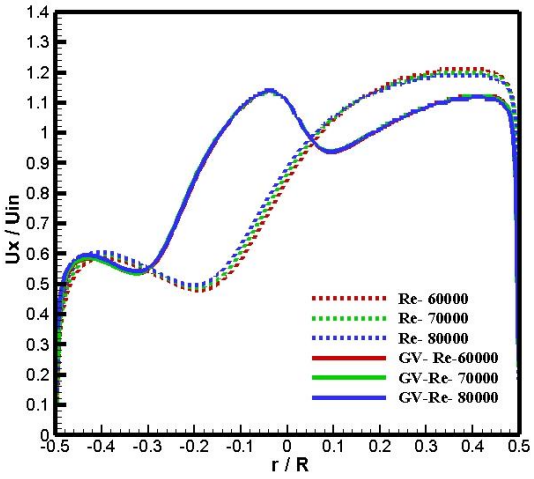

Figure 8 Speed profile graph

Figure 9 illustrates the normalized average velocity profile (U) at various Reynolds numbers in a 90° pipe bend cross-section without guide vanes. The points SP, RP, and MID represent the separation point, reattachment point, and midpoint, respectively. Fluid velocity depiction occurs in the outer core of the pipe bend. In scenarios without guide vanes in the 90° pipe bend, the velocity profile on the inner core side indicates flow separation, characterized by decreased velocity, with regions exhibiting negative velocity. Meanwhile, the separation point is identified through a zone with reduced velocity. The reversal of the velocity profile towards the positive direction serves to identify the reattachment point.

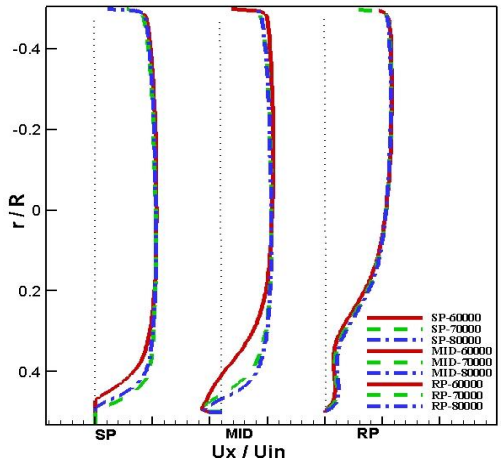

Figure 9 Normalized velocity profiles at various locations within the curved pipe and across different Reynolds numbers

4. Separation and Reattachment location

Figure 10 illustrates the initial separation point of fluid flow in a 90° pipe bend without guide vanes. This section highlights the points where flow separation occurs. The method for identifying and measuring separation and reattachment points in this study is like the research conducted in [15]. Data collection is performed at the initial point of separation occurrence, with varying values of x and y. Subsequently, the angular position is obtained for each Reynolds number $\left(\alpha = arc\left(\frac{y}{x}\right) \times \frac{180}{\pi}\right)$. The separation points at each Reynolds number are α = 72.45°, 74.32°, and 75.87°, respectively. Based on the presented location data, it is evident that the separation angle α increases with the increasing Reynolds number used.

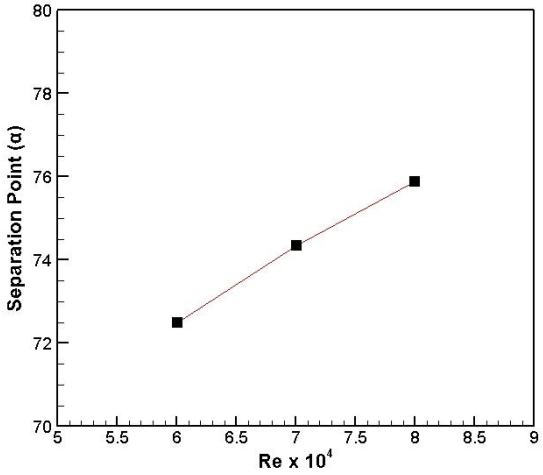

Figure 10 pipe bend separation point 90° none guide vane

Figure 11 depicts the initial reattachment points of fluid flow after passing through a pipe bend. Data collection is conducted at the initial reattachment point, with varying x values for each data point. Here, the value of X = position on x - diameter of the pipe bend, representing the reattachment point for each data point (X/D). The reattachment points for each Reynolds number are 0.354, 0.335, and 0.303, respectively. Changing the Reynolds number does not significantly affect the reattachment location. However, fluid flow

reintegrates more rapidly with increasing Reynolds number.

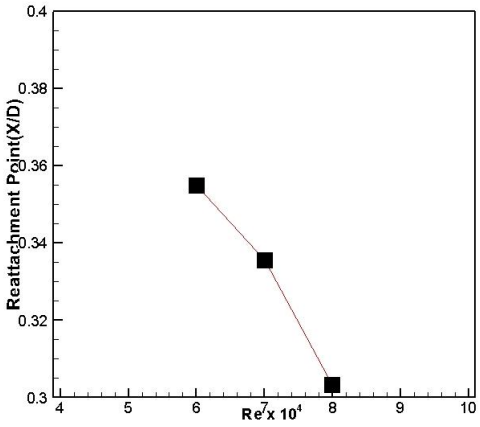

Figure 11 reattachment points pipe bend 90° none guide vane

Figure 12 depicts the cross-sectional velocity contour of the outlet pipe bend, normalized by the inlet velocity. Among the three Reynolds numbers examined significant disparities in velocity contours are observed between the 90° pipe bend devoid of a guide vane and the 90° pipe bend equipped with a guide vane. Within the velocity distribution of the 90° pipe bend devoid of a guide vane, there is an evident area of reduced fluid velocity near the inner core, with an increase in velocity as it approaches the outer core. In contrast, the presence of a guide vane results in a pronounced modification of the velocity contours. Moreover, using a guide vane promotes a more homogeneous fluid velocity distribution across the inner and outer core regions. This uniform distribution becomes progressively conspicuous with increasing Reynolds numbers. Furthermore, there is an absence of low-velocity zones in the velocity contour of the 90° pipe bend when equipped with a guide vane.

Figure 13 displays the contour of the x-velocity. In the 90° pipe bend without a guide vane, a noticeable transparent area of low velocity is observed after the flow passes through the bend. This observation signifies the occurrence of fluid flow separation. The utilization of a guide vane can effectively eliminate this fluid flow separation by redirecting the flow toward the inner core region.

5. Conclusions

This study employs a guide vane to mitigate flow separation in fluid flow characteristics through a 90° pipe bend. The research utilizes the k-epsilon turbulence model, investigating Reynolds numbers of $6 \times 10^4, 7 \times 10^4, and\ 8 \times 10^4$. The impact of the Reynolds number on fluid velocity profile characteristics is minimal. The α separation on the 90° pipe bend without a guide vane increases as the Reynolds number rises. Additionally, increasing Reynolds number accelerates fluid flow, resulting in reattachment. A negative velocity region indicates flow separation in the 90° pipe bend without a guide vane, a low-velocity region marks the separation point, and reattachment is confirmed by the return of the velocity profile in the positive direction. Using a guide vane improves the velocity profile within the -0.34 ≤ r/R ≤ -0.05 range. Concurrently, the guide vane ensures a more even distribution of fluid velocity between the inner core and outer core. This uniformity becomes more pronounced with higher Reynolds numbers. Furthermore, applying a guide vane eliminates fluid flow separation in the 90° pipe bend with a ratio $\frac{R_c}{D} \leq 1.5$. The guide vane aligns fluid flow, preventing the formation of low-velocity regions, controlling fluid flow velocity, and reducing turbulence during abrupt changes in flow direction or rapid velocity changes. Additionally, the guide vane directs fluid flow toward the inner core, enhancing the velocity and pressure distribution in the pipe to prevent flow separation[17].

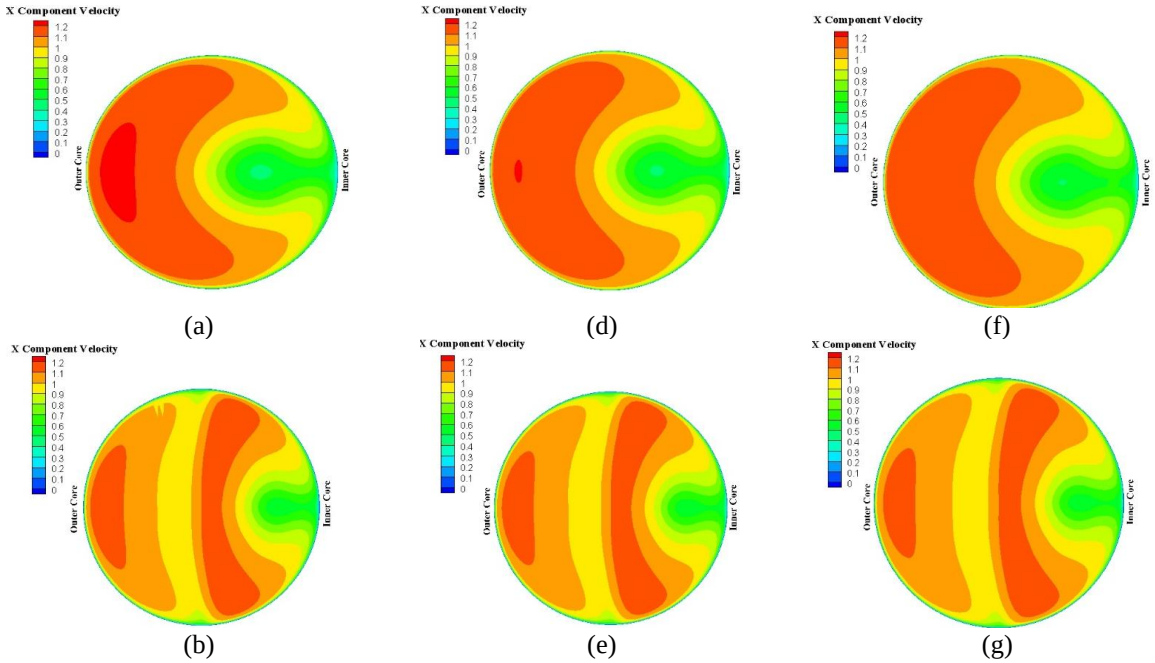

Figure 12 Velocity contour at the exit of a 90° pipe bend with none guide vane and using guide vane $Re = 6 \times 10^4$ (a) none guide vane (b) using guide vane, $Re = 7 \times 10^4$ (d) none guide vane (e) using guide vane, $Re = 8 \times 10^4$ (f) none guide vane (g) using guide vane

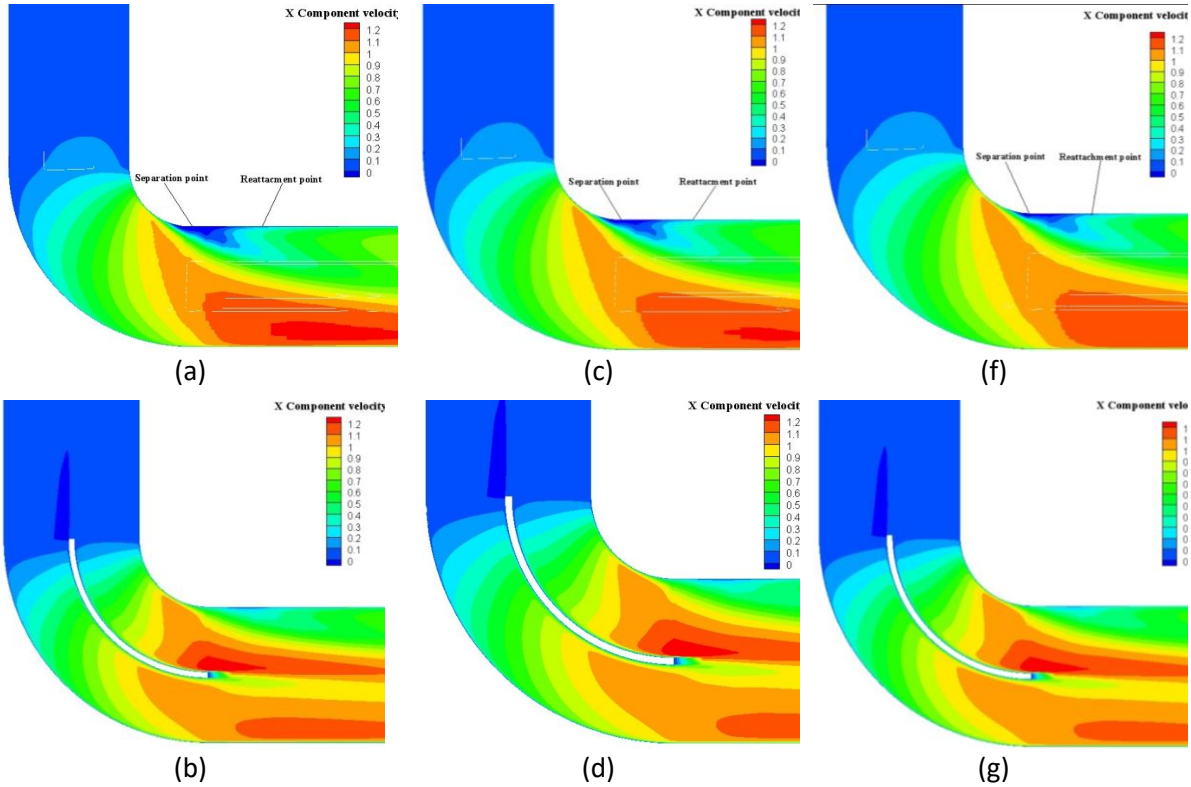

Figure 13 Velocity contour along the pipe at $Re = 6 \times 10^4$ (a) none guide vane (b) using guide vane, $Re = 7 \times 10^4$ (c) none guide guide vane (d) using guide vane, $Re = 8 \times 10^4$ (f) none guide vane (g) using guide vane

Reference

[1] H. Harinaldi, A. S. Wibowo, J. Julian, and B. Budiarso, "The comparison of an analytical, experimental, and simulation approach for the average induced velocity of a dielectric barrier discharge (DBD)," in *AIP Conference Proceedings*, AIP Publishing, 2019.

[2] J. Julian, W. Iskandar, F. Wahyuni, and N. T. Bunga, "Aerodynamic Performance Improvement on NACA 4415 Airfoil by Using Cavity," *Jurnal Asiimetrik: Jurnal Ilmiah Rekayasa Dan Inovasi*, pp. 135–142, 2023.

[3] J. Julian, W. Iskandar, F. Wahyuni, and F. Ferdyanto, "Computational Fluid Dynamics Analysis Based on The Fluid Flow Separation Point on The Upper Side of The NACA 0015 Airfoil With The Coefficient of Friction," *Media Mesin: Majalah Teknik Mesin*, vol. 23, no. 2, pp. 70–82, 2022.

[4] J. Julian, Harinaldi, Budiarso, C.-C. Wang, and M.-J. Chern, "Effect of plasma actuator in boundary layer on flat plate model with turbulent promoter," *Proc Inst Mech Eng G J Aerosp Eng*, vol. 232, no. 16, pp. 3001–3010, 2018.

[5] J. Julian, W. Iskandar, F. Wahyuni, A. Armansyah, and F. Ferdyanto, "Effect of Single Slat and Double Slat on Aerodynamic Performance of NACA 4415," *International Journal of Marine Engineering Innovation and Research*, vol. 7, no. 2, 2022.

[6] J. Julian and R. F. Karim, "Flow control on a squareback model," *International Review of Aerospace Engineering*, vol. 10, no. 4, pp. 230–239, 2017.

[7] Q. Xu, X. Yuan, C. Liu, X. Wang, and L. Guo, "Signal selection for identification of multiphase flow patterns in offshore pipeline-riser system," *Ocean Engineering*, vol. 268, p. 113395, 2023.

[8] J. Julian, W. Iskandar, and F. Wahyuni, "ANALYSIS OF AERODYNAMIC PERFORMANCE OF EROSION AIRFOIL WITH REYNOLDS NUMBER VARIATIONS," *Jurnal Ilmiah Teknologi dan Rekayasa*, vol. 28, no. 2, pp. 102–116, 2023.

[9] M. S. Medeiros Jr and L. G. Ribeiro, "Micromechanical elastoplastic limit analysis of in-plane bending of Functionally Graded Pipe elbows," *Thin-Walled Structures*, vol. 171, p. 108778, 2022.

[10] J. Julian, W. Iskandar, and F. Wahyuni, "HYDRODYNAMICS ANALYSIS OF JANUS SPHERE AT VARIATIONS OF THE REYNOLDS NUMBER," *J Teknol*, vol. 15, no. 2, pp. 315–324, 2023.

[11] S. Wegt, R. Maduta, J. Kissing, J. Hussong, and S. Jakirlić, "LES-based vortical flow characterization in a 90-turned pipe bend," *Comput Fluids*, vol. 240, p. 105418, 2022.

[12] J. Julian, W. Iskandar, F. Wahyuni, and N. T. Bunga, "Characterization of the Co-Flow Jet Effect as One of the Flow Control Devices," *Jurnal Asiimetrik: Jurnal Ilmiah Rekayasa Dan Inovasi*, pp. 185–192, 2022.

[13] A. Kalpakli Vester, S. S. Sattarzadeh, and R. Örlü, "Combined hot-wire and PIV measurements of a swirling turbulent flow at the exit of a 90° pipe bend," *J Vis (Tokyo)*, vol. 19, pp. 261–273, 2016.

[14] K. Sudo, M. Sumida, and Hje. Hibara, "Experimental investigation on turbulent flow in a circular-sectioned 90-degree bend," *Exp Fluids*, vol. 25, no. 1, pp. 42–49, 1998.

[15] P. Dutta, S. K. Saha, N. Nandi, and N. Pal, "Numerical study on flow separation in 90° pipe bend under high Reynolds number by k-ε modelling," *Engineering Science and Technology, an International Journal*, vol. 19, no. 2, pp. 904–910, 2016.

[16] J. Kim, M. Yadav, and S. Kim, "Characteristics of secondary flow induced by 90-degree elbow in turbulent pipe flow," *Engineering Applications of Computational Fluid Mechanics*, vol. 8, no. 2, pp. 229–239, 2014.
[17] R. Reghunathan Valsala, S. W. Son, A. Suryan, and H. D. Kim, "Study on reduction in pressure losses in pipe bends using guide vanes," *J Vis (Tokyo)*, vol. 22, no. 4, pp. 795–807, 2019, doi: 10.1007/s12650-019-00561-w.
[18] S. KUMAR SAHA and N. Nandi, "Change in Flow Separation and Velocity Distribution Due to Effect of Guide Vane Installed in a 90° Pipe Bend.," *Mechanics & Mechanical Engineering*, vol. 21, no. 2, 2017.
[19] Y. Du and J. A. Ekaterinaris, "Time-marching schemes for spatially high order accurate discretizations of the Euler and Navier–Stokes equations," *Progress in Aerospace Sciences*, vol. 130, p. 100795, 2022.
[20] M. T. A. Fadli, G. Marausna, F. Jayadi, G. D. A. Larasati, V. A. Victoria, and A. R. Ramadhan, "Rancang Bangun Visualisasi Aliran Air di Dalam Pipa Tubular dengan Vortex Generator untuk Meningkatkan Sifat Turbulensi Fluida," *Teknika STTKD: Jurnal Teknik, Elektronik, Engine*, vol. 7, no. 2, pp. 205–215, 2021.
[21] G. F. Homicz, "Computational Fluid Dynamic simulations of pipe elbow flow.," Sandia National Laboratories (SNL), Albuquerque, NM, and Livermore, CA …, 2004.
[22] J. Julian, F. Wahyuni, W. Iskandar, and R. Ramadhani, "The effect of curvature ratio towards the fluid flow characteristics in bend pipe based on numerical methods," *Turbo: Jurnal Program Studi Teknik Mesin*, vol. 12, no. 1, 2023.
[23] W. Iskandar, "Study of Airfoil Characteristics on NACA 4415 with Reynolds Number Variations," *International Review on Modelling and Simulations (IREMOS)*, vol. 15, no. 3, pp. 162–171, 2022.